Bioorganic & Medicinal Chemistry 18 (2010) 6249–6257

Contents lists available at ScienceDirect

Bioorganic & Medicinal Chemistry

journal homepage: www.elsevier.com/locate/bmc

The unsaturated acyclic nucleoside analogues bearing a sterically constrained (*Z*)-4′-benzamido-2′-butenyl moiety: Synthesis, X-ray crystal structure study, cytostatic and antiviral activity evaluations

Krešimir Benci [a], Karlo Wittine [a], Malajka Radan [a], Mario Cetina [b], Mirela Sedić [c], Sandra Kraljević Pavelić [d], Krešimir Pavelić [d], Erik De Clercq [e], Mladen Mintas [a,*]

[a] Department of Organic Chemistry, Faculty of Chemical Engineering and Technology, University of Zagreb, Maruličev trg 19, 10000 Zagreb, Croatia
[b] Department of Applied Chemistry, Faculty of Textile Technology, University of Zagreb, Prilaz baruna Filipovića 28a, 10000 Zagreb, Croatia
[c] Division of Molecular Medicine, Laboratory for Systems Biomedicine, Ruđer Bošković Institute, Bijenička cesta 54, PO Box 1016, 10001 Zagreb, Croatia
[d] Department of Biotechnology, University of Rijeka, Trg braće Mažuranića 10, 51000 Rijeka, Croatia
[e] Rega Institute for Medical Research, Katholieke Universiteit Leuven, Minderbroedersstraat 10, B-3000 Leuven, Belgium

ARTICLE INFO

Article history:
Received 22 April 2010
Revised 7 July 2010
Accepted 15 July 2010
Available online 7 August 2010

Keywords:
Unsaturated acyclic nucleoside analogues
X-ray diffraction
Supramolecular self-assembling
Cytostatic activity
Antiviral activity

ABSTRACT

A series of the novel acyclic unsaturated pyrimidine (**1**–**12**) and adenine (**13**) nucleoside analogues bearing conformationally restricted (*Z*)-2′-butenyl moiety were synthesized and evaluated for their antiviral and cytostatic activity potency against malignant tumor cell lines and normal human fibroblast (WI38). The N-1 and/or N-3 acyclic side chain substitution in pyrimidine ring in N-3 substituted 5-trifluoromethyluracil derivative (**11**), N-1, N-3 disubstituted 5-fluorouracil derivative (**12**) and adenine derivative (**13**) was deduced from their ^{1}H and ^{13}C NMR spectra and confirmed by single crystal X-ray structure analysis. The X-ray crystal structure analysis **11**–**13** revealed also supramolecular self-assemblies, in which infinite chains or dimers built two- and three-dimensional networks. The results of the in vitro cytostatic activity evaluations of **1**–**13** indicate that the majority of the compounds tested exhibited a non-specific and moderate antiproliferative effect at the highest concentration (100 μM). Of all evaluated compounds on the cell lines tested only the N-1 4″-fluoro-substituted-benzamide uracil derivative (**7**) showed rather marked and selective inhibitory activity against the growth of MCF-7 cells at a concentration of 2.7 μM and no cytotoxic effect on normal fibroblasts WI38. This compound can be therefore considered as a potential antitumor lead compound for further synthetic structure modification.

1. Introduction

Nucleoside analogues have been the cornerstone of antiviral chemotherapy over the past decades.[1] Although structure–activity relationship studies have not led to a uniform pharmacophore model for the antiviral activities of nucleosides, particular structural features such as the presence of unsaturated acyclic side chain as a substitute for nucleosides sugar have proved to be effective for specific antiviral activities.[2] The diverse range of compounds containing this structural motif includes the anti-HIV agent carbovir,[3] the antibiotic neplanocin A[4] and many other examples of such type of compounds with significant antiviral or antibacterial activity. Furthermore, the introduction of a rigid structural element into nucleoside or carbocyclic nucleoside structure have been shown to lead to synthesis of effective antiviral nucleoside analogues.[5,6] Thus, the presence of a double bond in acyclic nucleoside analogues is a structural feature important for strong antiherpetic activity of the guanine analogue.[7] Thymidine with a 2′-butenyl spacer was the first acyclic nucleoside analogue exhibiting potent inhibition of thymidine kinase 2 (*TK-2*) which catalyzed phosphorylation of antiviral drugs.[8] Among them, (*Z*)-configuration of the cyclopropyl guanine nucleoside showed antiherpetic potency (HSV-1 and HSV-2) comparable to that of acyclovir.[9]

In this connection and related to our previous studies on acyclic nucleoside analogues[2,10] we prepared a series of the novel *cis*-olefinic pyrimidine (**1**–**12**) and adenine (**13**) nucleoside analogues (Fig. 1). The initial aim of this study was to evaluate the antiviral activity potency of this new type of acyclic nucleoside analogues as well as their inhibitory activities against human tumor cell lines. Besides, we also wanted to examine by X-ray crystal structure analysis how the fluorinated pyrimidine (**11** and **12**) nucleoside bases and its adenine (**13**) analogue influence the formation of supramolecular self-assembling which play an important role in drug receptor interactions.

* Corresponding author. Tel.: +385 1 4597 214; fax: +385 1 4597 224.
E-mail addresses: mladen.mintas@fkit.hr, mmintas@fkit.hr (M. Mintas).

0968-0896/$ - see front matter © 2010 Elsevier Ltd. All rights reserved.
doi:10.1016/j.bmc.2010.07.035

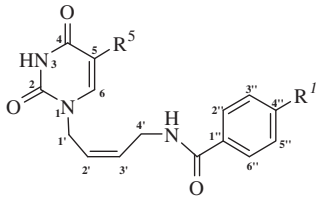

1-4 and **7,8**

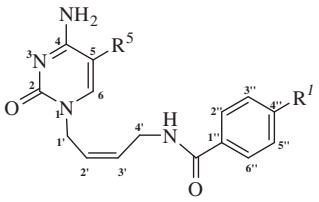

5,6 and **9,10**

	1	2	3	4	5	6	7	8	9	10
R^5	H	F	CH_3	CF_3	H	F	H	CH_3	H	F
R^1	H	H	H	H	H	H	F	F	F	F

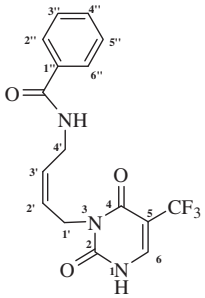

11

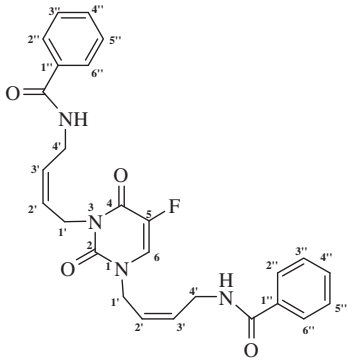

12

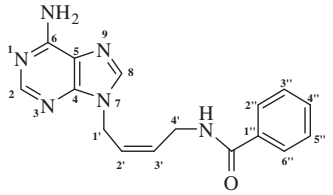

13

Figure 1. The benzamide derivatives of unsaturated acyclic pyrimidine (**1**–**12**) and adenine (**13**) nucleoside analogues.

2. Results and discussion

2.1. Chemistry

The new unsaturated acyclic uracil (**1–4**, **7**, and **8**), cytosine (**5**, **6**, **9**, and **10**) and adenine (**13**) nucleoside analogues bearing a conformationally restricted (*Z*)-2′-butenyl moiety were synthesized by condensation of nucleoside bases with (*Z*)-4-chloro-2-butenylbenzamide (**15**) or (*Z*)-4-chloro-2-butenyl-4-fluorobenzamide (**16**), respectively (Scheme 1). These precursors were readily prepared by reaction of (*Z*)-4′-chloro-2′-butenylamine hydrochloride (**14**) with benzamide or 4-fluorobenzamide. Besides N-1 regioselectivity of the coupling of heterocycle with acyclic residue which is considered essential as natural pyrimidine nucleosides are substituted at N-1, the N-3 substitution has also been found in the N-3 alkylated 5-trifluoromethyluracil derivative **11** as well as the N-1 and N-3 dialkylated 5-fluorouracil derivative **12**.

2.2. ^{1}H and ^{13}C NMR spectra

Structures of the newly synthesized compounds were deduced by analysis of their ^{1}H and ^{13}C NMR as well as mass spectra. The assignment of ^{1}H NMR spectra was performed on the basis of the chemical shifts, substituent-induced chemical shifts, and signal intensities, magnitude and multiplicity of H–H coupling constants. The ^{1}H and ^{13}C NMR data given in Table 1 and the experimental part are in full agreement with the proposed structures. DMSO-d_6 was used as a solvent for all compounds; chemical shifts are referred to TMS.

2.3. X-ray crystal structure analysis

The single X-ray crystal structure analysis of 5-trifluoromethyluracil derivative (**11**), N-1, N-3-dialkylated 5-fluorouracil derivative (**12**) and adenine derivative (**13**) was undertaken primarily to determine the position of nitrogen substitution in the pyrimidine ring of (**11**) and (**12**) and to examine the ability of those compounds to form supramolecular self-assembling. The molecular structures of **11** and **12** are shown in Figures 2 and 3. Equivalent bond lengths in N-3 substituted carboxamide derivative **11** and N-1, N-3 disubstituted derivative **12** are within the range in closely related 2-butenyl uracil derivatives,[11,12] and thymine derivative of 1-aminocyclopropane-1-carboxylic acid we published previously.[12] Butenyl moiety adopts *cis* conformation in these two structures; the C7–C8–C9–C10 torsion angle in **11** amounts −1.9(3)°, while the C7–C8–C9–C10 and C18–C19–C20–C21 torsion angles in **12** are 1.4(2) and 5.1(2)°, respectively.

The biggest conformational difference between these two structures is in the orientation of the carboxamide moiety. The conformation of this moiety in **11**, defined by the C9–C10–N2–C11 torsion angle of 127.08(17)°, is anticlinal. In **12**, two carboxamide moieties have two different conformations, synclinal and anticlinal [C9–C10–N2–C11 = 78.47(17)°; C20–C21–N4–C22 = −143.90(14)°]. The 2-butenyl-benzamido moiety attached to the N3 atom of the pyrimidine ring in **11** has different orientation compared to **12**, which is accompanied by formation of intramolecular hydrogen bonds between moiety and ring (Figs. 2 and 3).

The molecules of N-3 trifluoromethyluracyl derivative **11** are assembled by N1···O3 hydrogen bond [D···A = 2.737(3) Å] into infinite chains which can be described by graph-set notation as $C(6)$[13] (Fig. 4). This hydrogen bond is reinforced by C6···O1 hydrogen bond [D···A = 3.460(2) Å], so forming new chain motif and hydrogen-bonded sheets.

The sheets are further linked by two weak aromatic π···π stacking interactions[14] between nearly parallel pyrimidine and phenyl rings of the neighboring molecules. An interplanar angle (α) between the rings is 9.90(10)°. These two π···π interactions form dimers and a complete two-dimensional network.

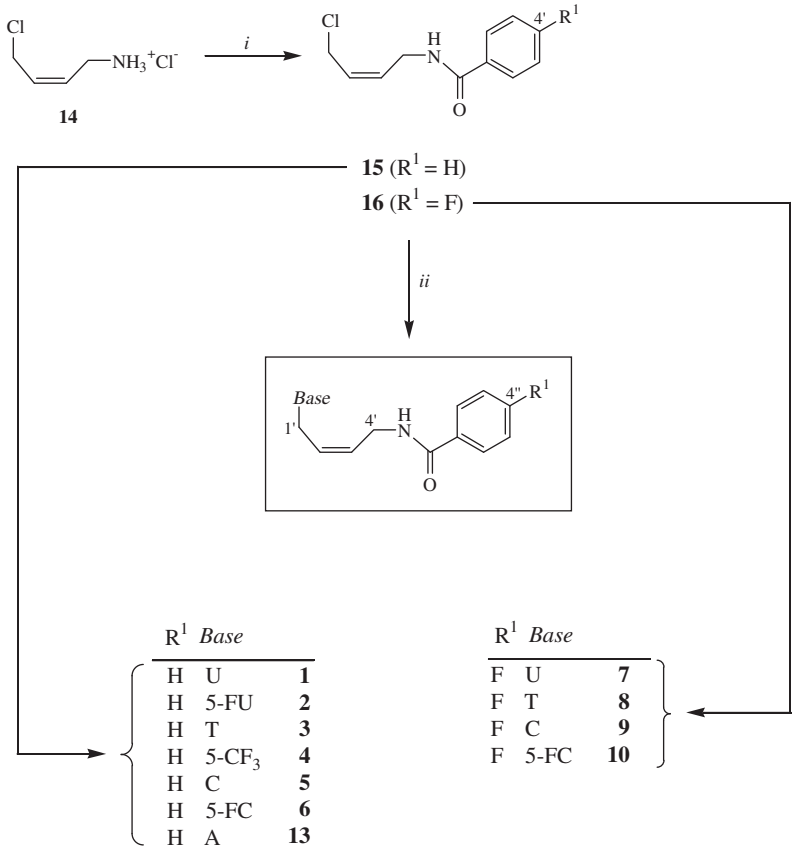

Scheme 1. Synthesis of carboxamide derivatives of unsaturated acyclic uracil (**1**–**4**, **7**, and **8**), cytosine (**5**, **6**, **9**, and **10**), and adenine (**13**) nucleoside analogues. Reagents and conditions: (i) THF, H_2O, benzoylchloride or 4-fluorobenzoylchloride, rt; (ii) uracil (U), 5-fluorouracil (5-FU), 5-trifluoromethyluracil (5-CF_3U), thymine (T), cytosine (C), 5-fluorocytosine (5-FC) or adenine (A), DMF, NaH, rt.

Table 1
^{1}H NMR chemical shifts (δ/ppm) and H–H coupling constants (J/Hz) in ^{1}H NMR spectra for compounds **1**–**13** (c.f. Fig. 1)

	H-3	H-5	H-6	H-1′	H-2′	H-3′	H-4′	NH	H-3″	H-2″	H-4″	NH_2
1	11.27 (br, 1H)	5.58 (d, 1H, J_3 = 7.83)	7.69 (d, 1H, J_3 = 7.86)	4.45 (d, 2H, J_3 = 6.72)	5.65 (m, 1H)	5.53 (m, 1H)	4.03 (t, 2H, J_3 = 5.87)	8.70 (br, 1H)	7.85 (d, 2H, J_3 = 6.87)	7.46 (t, 2H, J_3 = 7.08)	7.52 (d, 1H, J_3 = 6.99)	/
2	11.71 (br, 1H)	/	8.15 (d, 1H, J_3 = 6.72)	4.43 (d, 2H, J_3 = 6.84)	5.68 (m, 1H)	5.53 (m, 1H)	4.02 (t, 2H, J_3 = 6.00)	8.81 (br, 1H)	7.87 (d, 2H, J_3 = 7.38)	7.46 (t, 2H, J_3 = 7.00)	7.53 (d, 1H, J_3 = 7.26)	/
3[a]	11.26 (br, 1H)	/	7.59 (s, 1H)	4.41 (d, 2H, J_3 = 6.78)	5.67 (m, 1H)	5.50 (m, 1H)	4.03 (t, 2H, J_3 = 5.92)	8.72 (br, 1H)	7.85 (d, 2H, J_3 = 7.08)	7.46 (t, 2H, J_3 = 7.13)	7.52 (d, 1H, J_3 = 6.93)	/
4	11.86 (br, 1H)	/	8.46 (s, 1H)	4.55 (d, 2H, J_3 = 6.73)	5.66 (m, 1H)	5.58 (m, 1H)	4.20 (t, 2H, J_3 = 5.97)	8.75 (br, 1H)	7.85 (d, 2H, J_3 = 6.84)	7.47 (t, 2H, J_3 = 7.11)	7.53 (d, 1H, J_3 = 6.96)	/
5	/	5.67 (d, 1H, J_3 = 7.14)	7.63 (d, 1H, J_3 = 7.14)	4.43 (d, 2H, J_3 = 6.75)	5.63 (m, 1H)	5.52 (m, 1H)	4.04 (t, 2H, J_3 = 5.97)	8.71 (br, 1H)	7.86 (d, 2H, J_3 = 6.87)	7.46 (t, 2H, J_3 = 7.14)	7.52 (d, 1H, J_3 = 6.96)	7.03 (br, 2H)
6	/	/	7.99 (d, 1H, J_3 = 6.72)	4.41 (d, 2H, J_3 = 6.84)	5.64 (m, 1H)	5.54 (m, 1H)	4.04 (t, 2H, J_3 = 5.97)	8.72 (br, 1H)	7.86 (d, 2H, J_3 = 6.81)	7.47 (t, 2H, J_3 = 7.14)	7.52 (d, 1H, J_3 = 6.96)	7.53 (br, 1H) + 7.40 (br, 1H)
7	11.27 (br, 1H)	5.57 (d, 1H, J_3 = 7.86)	7.67 (d, 1H, J_3 = 7.86)	4.44 (d, 2H, J_3 = 6.79)	5.65 (m, 1H)	5.55 (m, 1H)	4.02 (t, 2H, J_3 = 5.98)	8.72 (br, 1H)	7.91 (dd, 2H, J_{1-3} = 8.70; J_{2-4} = 8.70)	7.29 (t, 2H, J_3 = 8.79)	/	/
8[b]	11.27 (br, 1H)	/	7.59 (s, 1H)	4.42 (d, 2H, J_3 = 6.78)	5.65 (m, 1H)	5.53 (m, 1H)	4.03 (t, 2H, J_3 = 5.84)	8.75 (br, 1H)	7.93 (dd, 2H, J_{1-3} = 8.67; J_{2-4} = 8.67)	7.31 (t, 2H, J_3 = 8.84)	/	/
9	/	5.66 (d, 1H, J_3 = 7.14)	7.61 (d, 1H, J_3 = 7.14)	4.41 (d, 2H, J_3 = 6.84)	5.62 (m, 1H)	5.49 (m, 1H)	4.02 (t, 2H, J_3 = 6.00)	8.74 (br, 1H)	7.92 (dd, 2H, J_{1-3} = 8.70; J_{2-4} = 8.70)	7.29 (t, 2H, J_3 = 8.79)	/	7.05 (br, 1H) + 6.97 (br, 1H)
10	/	/	7.98 (d, 1H, J_3 = 6.69)	4.40 (d, 2H, J_3 = 6.75)	5.64 (m, 1H)	5.53 (m, 1H)	4.03 (t, 2H, J_3 = 5.93)	8.75 (br, 1H)	7.93 (dd, 2H, J_{1-3} = 8.61; J_{2-4} = 8.61)	7.30 (t, 2H, J_3 = 8.81)	/	7.62 (br, 1H) + 7.40 (br, 1H)
11[c]	/	/	8.15 (d, 1H, J_3 = 6.72)	4.43 (m, 2H)	5.68 (m, 1H)	5.53 (m, 1H)	4.02 (m, 2H)	8.81 (br, 1H)	7.87 (d, 2H, J_3 = 7.38)	7.46 (tm, 2H)	7.53 (m, 1H)	/
12	/	/	8.15 (s, 2H)	4.43 (m, 4H)	5.68 (m, 2H)	5.53 (m, 2H)	4.02 (m, 4H)	8.81 (br, 2H)	7.87 (d, 4H, J_3 = 7.38)	7.46 (tm, 4H)	7.53 (m, 2H)	/
13[d]	/	/	/	4.94 (d, 2H, J_3 = 6.30)	5.71 (m, 1H)	5.68 (m, 1H)	4.14 (t, 2H, J_3 = 5.28)	8.78 (br, 1H)	7.86 (d, 2H, J_3 = 6.78)	7.48 (t, 2H, J_3 = 8.67)	7.50 (d, 1H, J_3 = 6.70)	7.22 (br, 2H)

[a] Compound **3**: signal for $-CH_3$: 1.75 ppm (s, 3H).
[b] Compound **8**: signal for $-CH_3$: 1.76 ppm (s, 3H).
[c] Compound **12**: signal for H-1: 8.37 ppm (br, 1H).
[d] Compound **13**: signal for H-2: 8.18 ppm (s, 1H); signal for H-8: 8.15 ppm (s, 1H).

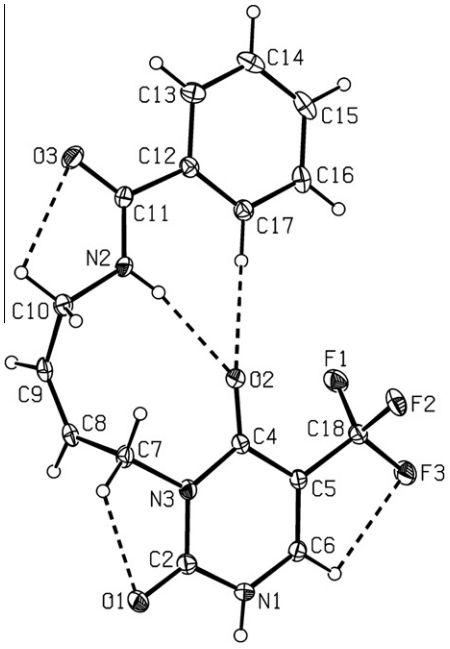

Figure 2. A molecular structure of **11**, with the atom-numbering scheme. Displacement ellipsoids for nonhydrogen atoms are drawn at the 30% probability level. The intramolecular hydrogen bonds are shown dashed.

Two N–H···O hydrogen bonds, N2···O4 [D···A = 2.9244(17) Å] and N4···O2 [D···A = 2.9762(16) Å] link the molecules of the N-1, N-3 disubstituted 5-fluorouracil derivative **12** into *C*(4) and *C*(11) chains, respectively (Fig. 5). Supramolecular structure of **12** also contains two C–H···O hydrogen bonds, C18···O3 [D···A = 3.4615(17) Å] and C28···O2 [D···A = 3.482(2) Å], which link infinite chains into two-dimensional network. Four π···π stacking interactions between pyrimidine and phenyl rings (α = 3.49(7)°) and between neighboring phenyl rings (α = 9.00(8)°) complete a three-dimensional network.

Adenine derivative **13** (Fig. 6), in which 2′-butenyl-benzamido moiety is bound to the N9 atom of the adenine moiety crystallizes as monohydrate. Bond lengths in **13** are close to equivalent ones in structurally related compounds.[12,15,16] The exception is C4–C5 bond length in (*Z*)-methyl 1-{*N*-[(*tert*-butoxy)carbonyl]amino}-2-(6-aminopurine-9-yl)cyclopropanecarboxylate[16] which is ca. 0.03 Å shorter.

The molecules of **13** are linked into dimers by two N–H···N hydrogen bonds, N6···N7 [D···A = 3.090(2) Å] and N6···N1 [D···A = 2.949(2) Å]. Water molecule participates also in supramolecular aggregation as hydrogen-bonded acceptor via N2···O2 hydrogen bond [D···A = 2.965(2) Å], and as double donor via O2···N3 [D···A = 3.039(2) Å] and O2···O1 hydrogen bond [D···A = 2.828(2) Å], thus generating a two-dimensional network (Fig. 7). The sixmembered and fivemembered rings of neighboring purine moieties are nearly parallel, so enabling three π···π interactions′ formation (α = 0°; α = 2.16(7)°). A fourth π···π interaction between phenyl rings with an interplanar angle of 0° expands the two-dimensional network into a three-dimensional network (Fig. 7).

3. Biological results

3.1. Cytostatic activity

The compounds were evaluated for their antiproliferative effect against several malignant tumor cell lines: cervical carcinoma (HeLa), colorectal adenocarcinoma, metastatic (SW 620), pancreatic carcinoma (MiaPaCa-2), breast epithelial adenocarcinoma, metastatic (MCF-7), breast adenocarcinoma metastatic (SK-BR-3) and larynx carcinoma (HEp-2), and compared with their effects on the growth of normal human fibroblasts (WI38) (Table 2, Supplementary data).

The results of the in vitro cytostatic activity evaluations revealed that the majority of the acyclic pyrimidine (**1–10**) and adenine nucleoside analogues (**13**) exhibited a non-specific and moderate antiproliferative effect at the highest concentration (100 μM) on the tested cell line panel. Strikingly, some compounds sharing structural similarity differed in the selectivity of their cytostatic activities (Supplementary data). For example, among uracil derivatives compound **7** showed selective and rather marked inhibitory activity against the growth of the MCF-7 cells (IC_{50} = 2.7 ± 0.05 μM), whereas compound **1** exerted pronounced selective cytostatic activity on HeLa cells (IC_{50} = 4.9 ± 0.04). These compounds resulted to have diverse effects on the growth of normal human fibroblasts as well. Compound **7** showed no cytotoxicity on WI38 while compound **1** showed strong cytotoxic effect on this cell line (IC_{50} = 6.6 ± 0.05) It is however interesting that introduction of Fluor abolished cytotoxic effects of compound **7** on WI38 (Fig. 1, Supplementary data). Contrary, comparing compound **3** (bearing a CH_3 moiety) that showed high cytotoxicity on WI38 (4.3 ± 0.07) with a structurally related compound **8** where Fluor has been introduced, strong cytotoxic effect on WI38 (0.1 ± 0.08) has not been abolished.

And again, cytosine derivatives **5**, **6** and **9** all exerted a strong cytotoxic effect on WI38 while introduction of Fluor at two positions in compound **10** seems to abolish cytotoxicity in this cell line (Fig. 1, Supplementary material).

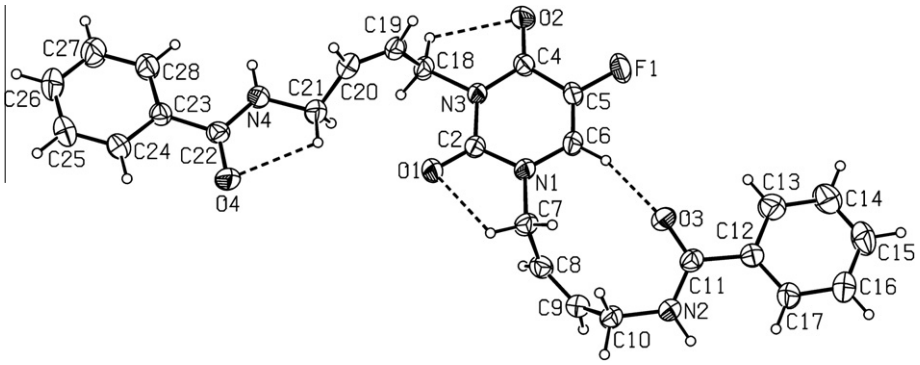

Figure 3. A molecular structure of **12**, with the atom-numbering scheme. Displacement ellipsoids for nonhydrogen atoms are drawn at the 30% probability level. The intramolecular hydrogen bonds are shown dashed.

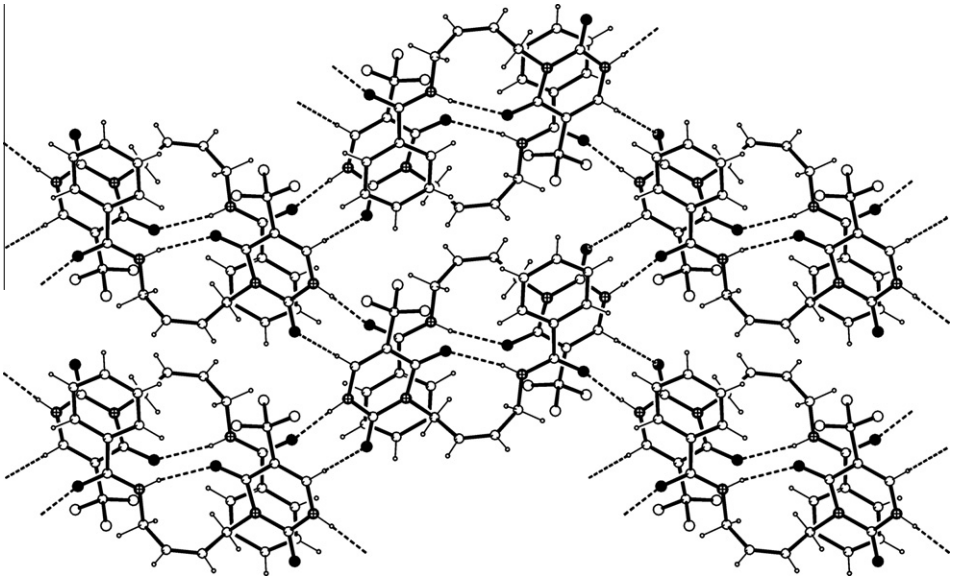

Figure 4. A part of the crystal structure of **11**, showing hydrogen bonds and pyrimidine and phenyl rings' stacking which form two-dimensional network. Hydrogen bonds are indicated by dashed lines.

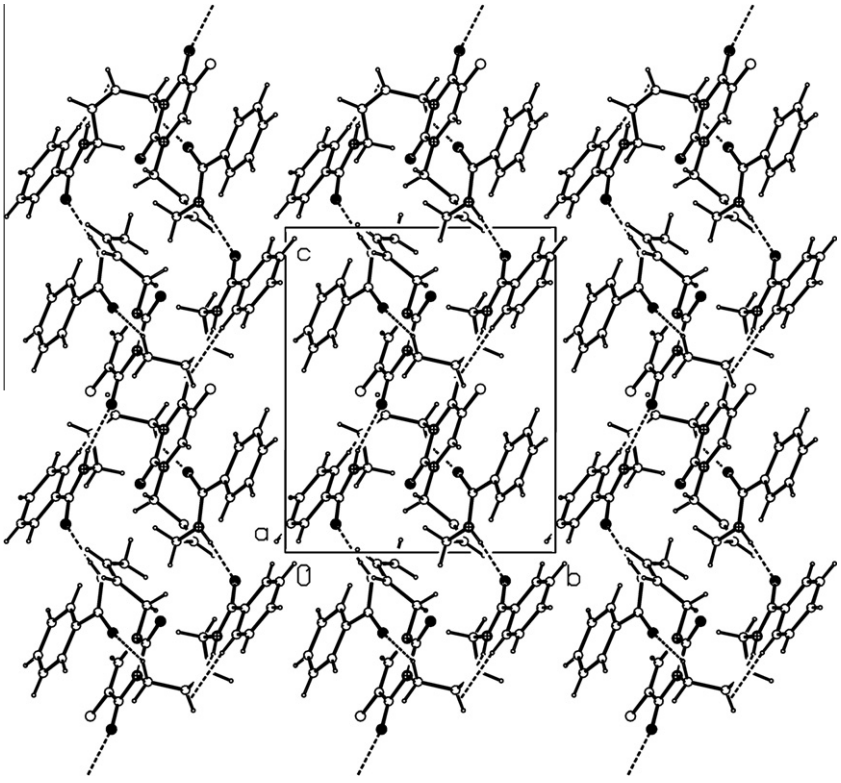

Figure 5. A crystal packing diagram of **12**, viewed along the *a* axis, and showing hydrogen bonds and parallel arrangements of pyrimidine and phenyl rings which enable three-dimensional network formation. Hydrogen bonds are indicated by dashed lines.

3.2. Antiviral activity

Compounds **1–10** and **13** were evaluated for their antiviral activity against a wide variety of DNA and RNA viruses, including HEL [herpes simplex virus type 1 (HSV-1) (KOS), HSV-2 (G), vaccinia virus, and vesicular stomatitis virus], Vero (parainfluenza-3, reovirus-1, Sindbis, Coxsackie B4, and Punta Toro virus), HeLa (vesicular stomatitis virus, Coxsackie virus B4, and respiratory syncytial virus) or MDCK [influenza A (H1N1; H3N2) and influenza B] viruses. Unfortunately, none of the compounds showed pronounced antiviral activity at subtoxic concentrations. Cytotoxicity of all evaluated compounds on HEL, Vero, HeLa, and MDCK cell cultures were greater then 100% (data not shown).

4. Conclusions

We have successfully prepared a series of the novel unsaturated acyclic pyrimidine (**1–12**) and adenine (**13**) nucleoside analogues

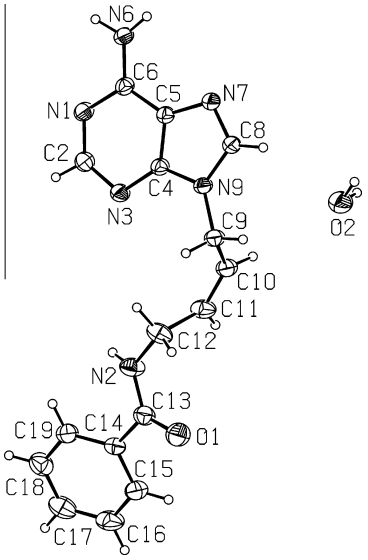

Figure 6. A molecular structure of monohydrate of compound **13**, with the atom-numbering scheme. Displacement ellipsoids for nonhydrogen atoms are drawn at the 30% probability level.

bearing a conformationally restricted (*Z*)-2′-butenyl moiety. X-ray structure analysis revealed supramolecular self-assemblies of 5-trifluoromethyluracyl derivative (**11**), N-1, N-3-dialkylated 5-fluorouracil derivative (**12**) and adenine derivative (**13**). In all of these structures, the main hydrogen-bonded motifs, chains or dimers, are extended into two-dimensional network (for **11**) or three-dimensional network (for **12** and **13**) by $\pi\cdots\pi$ interactions. The 4″-fluorosubstituted benzamide uracil derivative (**7**) showed selective cytostatic inhibitory activity in MCF-7 cell lines at micromolar concentrations and no cytotoxicity to human normal fibroblasts WI38. This compound would be therefore regarded as a potential antitumor lead compound for further synthetic structure modification.

5. Experimental

5.1. General methods

Melting points (uncorrected) were determined with Kofler micro hot-stage (Reichert, Wien). Precoated Merck Silica Gel 60F-254 plates were used for thin layer chromatography (TLC) and the spots were detected under UV light (254 nm). Column chromatography (CLC) was performed using silica gel (0.063–0.2 mm) Fluka; glass column was slurry-packed under gravity. The electron impact mass spectra were recorded with an EXTREL FT MS 2002 instrument with ionizing energy of 70 eV. ^{1}H and ^{13}C NMR spectra were obtained on a Bruker 300 MHz NMR spectrometer. All data were recorded in DMSO-d_6 at 298 K. Chemical shifts were referenced to the residual solvent signal of DMSO at δ 2.50 ppm for ^{1}H and δ 39.50 ppm for ^{13}C. Individual resonances were assigned on the basis of their chemical shifts, signal intensities, multiplicity of resonances, and H–H coupling constants.

5.2. Procedures for the preparation of compounds

5.2.1. General procedure for the preparation of (*Z*)-4-chloro-2-butenyl-benzamide (15) and (*Z*)-4-chloro-2-butenyl-4-fluorobenzamide (16)

To a stirred suspension of (*Z*)-4-chloro-2-butenylaminehydrochloride (**14**) (1.0 g, 7.0 mmol) in THF (35 ml) and water (0.2 ml) *N*,*N*-diisopropylethylamine (2.7 ml, 15.4 mmol) was added followed by addition of benzoylchloride (0.76 ml, 8.4 mmol) or 4-fluorobenzoylchloride (0.99 ml, 8.4 mmol). The resultant solution was stirred overnight at room temperature. Reaction mixture was evaporated, dissolved in CH_2Cl_2 (100 ml) and extracted with

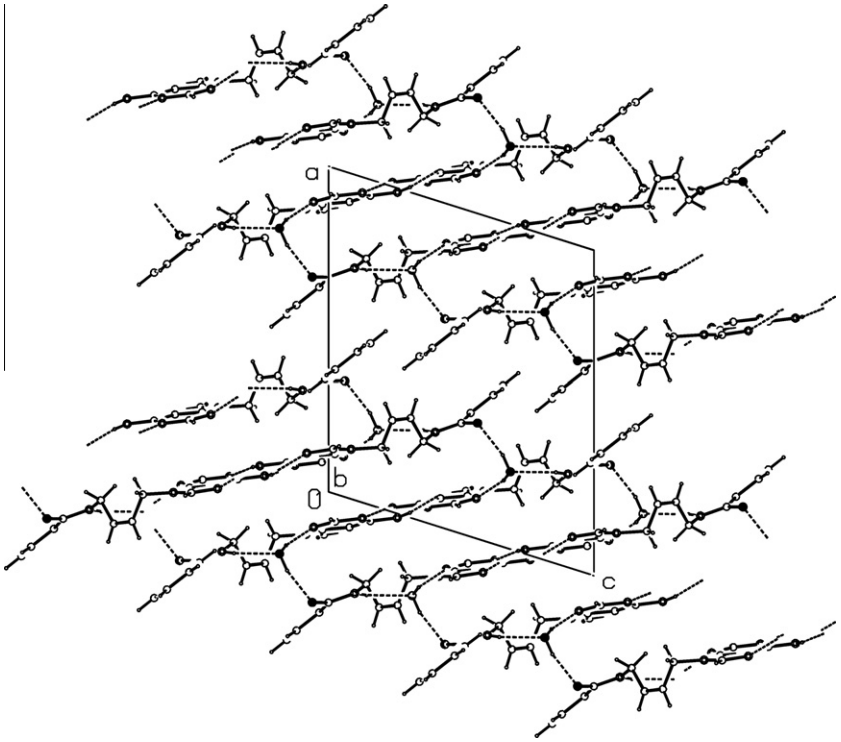

Figure 7. A crystal packing diagram of **13**, viewed along the *b* axis, and showing two-dimensional network formed by hydrogen bonds, which are extended by $\pi\cdots\pi$ interactions into three-dimensional network. Hydrogen bonds are indicated by dashed lines.

H_2O (4 × 20 ml), dried ($MgSO_4$), concentrated in vacuo. Purification by column chromatography (silica gel, PE/EtOAc = 3/1) afforded **15** (900 mg, 61%) and **16** (1100 mg, 69%) both as white crystals.

Compound **15**: ^{1}H NMR (DMSO) δ: 4.43 (d, 2H, J_3 = 6.84, H-1′); 5.68 (m, 1H, H-2′); 5.53 (m, 1H, H-3′); 4.02 (t, 2H, J_3 = 6.00, H-4′); 8.81 (br, 1H, NH); 7.87 (d, 2H, J_3 = 7.38, H-3″); 7.46 (d, 2H, J_3 = 7.00, H-2″); 7.53 (d, 1H, J_3 = 7.26, H-4″); ^{13}C NMR (DMSO) δ: 134.71 (C-1″), 131.71 (C-4″), 131.60 (C-2″), 128.88 (C-2′), 127.80 (C-3′), 125.82 (C-3″), 42.46 (C-1′), 36.81 (C-4′); mp = 51–53 °C.

Compound **16**: ^{1}H NMR (DMSO) δ: 4.41 (d, 2H, J_3 = 6.84, H-1′); 5.62 (m, 1H, H-2′); 5.49 (m, 1H, H-3′); 4.02 (t, 2H, J_3 = 6.00, H-4′); 8.74 (br, 1H, NH); 7.92 (dd, 2H, J_{1-3} = 8.70; J_{2-4} = 8.70, H-3″); 7.29 (d, 2H, J_3 = 8.79, H-2″); ^{13}C NMR (DMSO) δ: 166.13 (C-4″), 130.45 (C-2′), 131.27 and 131.22 (C-1″), 130.34 and 130.22 (C-3″), 127.43 (C-3′), 115.84 and 115.55 (C-2″), 94.12 (C-5), 42.75 (C-1′), 36.77 (C-4′); mp = 47–49 °C.

5.2.2. General procedure for the preparation of (*Z*)-1-(4′-benzamide-2′-butenyl)pyrimidine (1–6) and adenine (13) or (*Z*)-1-[4′-(4″-fluoro)benzamide-2′-butenyl]pyrimidine (7–10) derivatives

Compound **15** (210 mg, 1.0 mmol) or **16** (228 mg, 1.0 mmol) were added after 2 h to a stirred mixture containing pyrimidine or purine bases and NaH (1.2 equiv) in DMF (20 ml) the. Reaction mixture was then stirred overnight at room temperature. The resultant solution was concentrated to dryness in vacuo and purified by column chromatography (silica gel, CH_2Cl_2/MeOH = 20:1) which gave pure white crystals of pyrimidine (**1–12**) and adenine (**13**) derivatives.

5.2.3. Compounds preparation

5.2.3.1. (*Z*)-1-(4′-Benzamide-2′-butenyl)uracil (1). The procedure was carried out using uracil (448 mg, 4.0 mmol) which gave **1** (153 mg, 54%, mp = 143–157 °C). ^{13}C NMR (DMSO) δ: 166.67 (C═O), 164.17 (C-4), 151.39 (C-2), 145.72 (C-6), 134.77 (C-1″), 131.69 (C-4″), 131.50 (C-2″), 128.78 (C-2′), 127.63 (C-3′), 126.16 (C-3″), 101.67 (C-5), 44.54 (C-1′), 36.86 (C-4′); MS *m*/*z* 285.11 [MH]$^+$. Anal. ($C_{15}H_{15}N_3O_3$) C, H, N.

5.2.3.2. (*Z*)-1-(4′-Benzamide-2′-butenyl)-5-fluorouracil (2) and (*Z*)-1,3-di-(4′-benzamide-2′-butenyl)-5-fluorouracil (12). The procedure was carried out by using 5-fluorouracil (650 mg, 5.0 mmol) which gave **2** (145 mg, 48%, mp = 139–141 °C) and **12** (90 mg, 39%, mp = 152–154 °C).

Compound **2**: ^{13}C NMR (DMSO) δ: 166.66 (C═O), 158.17 and 157.83 (C-4), 150.11 (C-2), 138.68 (C-5), 134.71 (C-1″), 131.71 (C-4″), 131.60 (C-2″), 130.37 and 129.92 (C-6), 128.88 (C-2′), 127.80 (C-3′), 125.82 (C-3″), 44.70 (C-1′), 36.81 (C-4′); MS *m*/*z* 303.10 [MH]$^+$. Anal. ($C_{15}H_{14}FN_3O_3$) C, H, N.

Compound **12**: ^{13}C NMR (DMSO) δ: 166.21 (C═O), 157.87 and 156.54 (C-4), 151.34 (C-2), 139.08 (C-5), 134.21 (C-1″), 132.21 (C-4″), 131.83 (C-2″), 131.07 and 129.63 (C-6), 127.88 (C-2′), 126.92 (C-3′), 124.88 (C-3″), 44.74 (C-1′), 36.87 (C-4′); MS *m*/*z* 476.20 [MH]$^+$. Anal. ($C_{26}H_{25}FN_4O_4$) C, H, N.

5.2.3.3. (*Z*)-1-(4′-Benzamide-2′-butenyl)thymine (3). The procedure was carried out using thymine (504 mg, 4.0 mmol) which gave **3** (138 mg, 49%, mp = 130–138 °C). ^{13}C NMR (DMSO) δ: 166.59 (C═O), 164.70 (C-4), 151.33 (C-2), 141.49 (C-1″), 134.72 (C-6), 131.71 (C-4″), 131.46 (C-3″), 128.79 (C-2′), 127.61 (C-3′), 126.31 (C-2″), 109.25 (C-5), 44.14 (C-1′), 36.83 (C-4′); MS *m*/*z* 299.13 [MH]$^+$. Anal. ($C_{16}H_{17}N_3O_3$) C, H, N.

5.2.3.4. (*Z*)-1-(4′-Benzamide-2′-butenyl)-5-trifluoromethyluracil (4) and (*Z*)-3-(4′-benzamide-2′-butenyl)-5-trifluoromethyluracil (11). The procedure was carried out by using 5-trifluoromethyluracil (716 mg, 4.0 mmol) which gave **4** (151 mg, 43%, mp = 135–138 °C) and **11** (24 mg, 3.4%, mp = 131–133 °C).

Compound **4**: ^{13}C NMR (DMSO) δ: 166.66 (C═O), 152.17 and 150.83 (C-4), 150.11 (C-2), 140.90 (C-5), 134.71 (C-1″), 131.71 (C-4″), 131.60 (C-2″), 130.37 and 129.00 (C-6), 128.88 (C-2′), 127.80 (C-3′), 125.82 (C-3″), 44.70 (C-1′), 36.81 (C-4′); MS *m*/*z* 353.12 [MH]$^+$. Anal. ($C_{16}H_{14}F_3N_3O_3$) C, H, N.

Compound **11**: ^{13}C NMR (DMSO) δ: 166.40 (C═O), 152.20 and 150.74 (C-4), 150.15 (C-2), 140.70 (C-5), 134.75 (C-1″), 131.39 (C-4″), 131.20 (C-2″), 130.14 and 129.50 (C-6), 127.82 (C-2′), 127.30 (C-3′), 125.49 (C-3″), 44.30 (C-1′), 36.51 (C-4′); MS *m*/*z* 353.10 [MH]$^+$. Anal. ($C_{16}H_{14}F_3N_3O_3$) C, H, N.

5.2.3.5. (*Z*)-1-(4′-Benzamide-2′-butenyl)cytosine (5). The procedure was carried out by using cytosine (166 mg, 1.5 mmol) which gave **5** (123 mg, 43%, mp = 207–212 °C). ^{13}C NMR (DMSO) δ: 165.98 (C═O), 165.89 (C-4), 155.74 (C-2), 145.60 (C-6), 134.30 (C-1″), 131.15 (C-4″), 129.98 (C-2″), 128.26 (C-2′), 127.11 (C-3′), 126.90 (C-3″), 93.55 (C-5), 45.22 (C-1′), 36.20 (C-4′); MS *m*/*z* 284.13 [MH]$^+$. Anal. ($C_{15}H_{16}N_4O_2$) C, H, N.

5.2.3.6. (*Z*)-1-(4′-Benzamide-2′-butenyl)-5-fluorocytosine (6). The procedure was carried out by using cytosine (195 mg, 1.5 mmol) which gave **6** (152 mg, 50%, mp = 186–193 °C). ^{13}C NMR (DMSO) δ: 166.04 (C═O), 157.45 and 157.37 (C-4), 154.00 s (C-2), 134.28 (C-1″), 131.17 (C-4″), 130.37 (C-2″), 130.22 and 130.02 (C-6), 128.27 (C-2′), 127.10 (C-3′), 126.41 (C-3″), 136.46 (C-5), 45.25 (C-1′), 36.21 (C-4′); MS *m*/*z* 302.12 [MH]$^+$. Anal. ($C_{15}H_{15}FN_4O_2$) C, H, N.

5.2.3.7. (*Z*)-1-[4′-(4″-Fluoro)benzamide-2′-butenyl]uracil (7). The procedure was carried out by using uracil (448 mg, 4.0 mmol) which gave **7** (156 mg, 51%, mp = 151–154 °C).

^{13}C NMR (DMSO) δ: 165.97 (C═O), 165.59 (C-4″), 164.15 (C-4), 151.37 (C-2), 145.70 (C-6), 131.40 (C-2′), 131.25 and 131.21 (C-1″), 130.37 and 130.22 (C-3″), 126.21 (C-3′), 115.84 and 115.50 (C-2″), 101.66 (C-5), 44.53 (C-1′), 36.91 (C-4′); MS *m*/*z* 303.10 [MH]$^+$. Anal. ($C_{15}H_{14}FN_3O_3$) C, H, N.

5.2.3.8. (*Z*)-1-[4′-(4″-Fluoro)benzamide-2′-butenyl]thymine (8). The procedure was carried out by using thymine (504 mg, 4.0 mmol) which gave **8** (139 mg, 44%, mp = 199–204 °C). ^{13}C NMR (DMSO) δ: 166.00 (C═O), 165.54 (C-4″), 164.70 (C-4), 151.32 (C-2), 141.48 (C-6), 131.37 (C-3′), 131.32 and 131.25 (C-1″), 130.32 and 130.20 (C-3″), 126.37 (C-2′), 115.86 and 115.57 (C-2″), 109.25 (C-5), 44.14 (C-1′), 36.89 (C-4′); MS *m*/*z* 317.12 [MH]$^+$. Anal. ($C_{16}H_{16}FN_3O_3$) C, H, N.

5.2.3.9. (*Z*)-1-(4′-4″-Fluorobenzamide-2′-butenyl)cytosine (9). The procedure was carried out by using cytosine (166 mg, 1.5 mmol) which gave **9** (126 mg, 42%, mp = 187–197 °C). ^{13}C NMR (DMSO) δ: 166.39 (C═O), 166.00 (C-4″), 165.52 (C-4), 156.31 (C-2), 146.11 (C-6), 130.37 (C-2′), 131.25 and 131.21 (C-1″), 130.32 and 130.20 (C-3″), 127.43 (C-3′), 115.84 and 115.55 (C-2″), 94.12 (C-5), 44.75 (C-1′), 36.77 (C-4′); MS *m*/*z* 302.12 [MH]$^+$. Anal. ($C_{15}H_{15}FN_4O_2$) C, H, N.

5.2.3.10. (*Z*)-1-[4′-(4″-Fluoro)benzamide-2′-butenyl]-5-fluorocytosine (10). The procedure was carried out by using 5-fluorocytosine (195 mg, 1.5 mmol) which gave **10** (157 mg, 49%, mp = 170–174 °C). ^{13}C NMR (DMSO) δ: 165.97 (C═O), 165.51 (C-4″), 158.00 and 157.82 (C-4), 154.51 (C-2), 130.41 (C-6), 130.78 (C-2′), 131.25 and 131.22 (C-1″), 130.30 and 130.18 (C-3″), 126.96 (C-3′), 115.84 and 115.55 (C-2″), 137.76 (C-5), 44.77 (C-1′), 36.78 (C-4′); MS *m*/*z* 320.11 [MH]$^+$. Anal. ($C_{15}H_{14}F2N_4O_2$) C, H, N.

5.2.3.11. (*Z*)-9-(4′-Benzamide-2′-butenyl)adenine (13). The procedure was carried out by using adenine (203 mg, 1.5 mmol) which

gave **13** (139 mg, 45%, mp = 150–152 °C). ^{13}C NMR (DMSO) δ: 166.69 (C=O), 156.43 (C-4), 152.94 (C-8), 149.7 (C-6), 141.69 (C-2), 134.83 (C-1″), 131.69 (C-4″), 131.34 (C-3″), 128.78 (C-3′), 127.64 (C-2′), 131.34 (C-3″), 119.14 (C-5), 40.82 (C-1′), 36.85 (C-4′); MS *m*/*z* 308.14 $[MH]^+$. Anal. ($C_{16}H_{16}N_6O$) C, H, N.

5.3. X-ray determination of compounds 11, 12, and 13

Colorless single crystals of **11** and **12** suitable for X-ray single crystal analysis were obtained at room temperature by partial evaporation from a methanol solution. Colorless single crystal of **13** was obtained from an ethanol solution applying the same crystallization method. The intensities for **12** and **13** were collected at 295 K on a Oxford Diffraction Xcalibur2 diffractometer using graphite-monochromated Mo*K*α radiation (λ = 0.71073 Å). The intensities for **11** were collected on the same instrument at 130 K. *CrysAlis*[17] programs were used for data collection and reduction. The crystal structures were solved by direct methods.[18] All nonhydrogen atoms were refined anisotropically by full-matrix least-squares calculations based on F^2.[18] The hydrogen atoms of the N1 and N2 atoms in **11**, N2 and N4 atoms in **12**, and N2, N6 and O2 atoms in **13** were found in a difference Fourier map and their coordinates and isotropic thermal parameters have been refined freely. All other hydrogen atoms were included in calculated positions as riding atoms, with SHELXL97[18] defaults. Examination of the refined structure of **12** revealed that this structure contains solvent accessible void of 72.00 Å^3. This compound crystallizes with a solvent molecule which is severely disordered (the maximum electron density at the center of the void is 0.57 eÅ^{-3}), and could not be refined satisfactorily. The data are therefore corrected using the SQUEEZE routine in PLATON.[19] PLATON[19] program was used for structure analysis and drawings preparation. CCDC 773593–773595 contain the supplementary crystallographic data for this Letter. These data can be obtained free of charge from The Cambridge Crystallographic Data Centre via www.ccdc.cam.ac.uk/data_request/cif.

Crystal data for **11**: crystal dimension 0.17 × 0.26 × 0.70 mm^3; $C_{16}H_{14}F_3N_3O_3$, M_r = 353.30, monoclinic space group $P2_1/c$; a = 8.4391(6), b = 21.2803(18), c = 11.9798(10) Å, β = 133.542(5)°, V = 1559.5(2) Å^3; Z = 4; d_x = 1.505 g cm^{-3}; μ(MoKα) = 0.129 mm^{-1}; S = 0.976; R/wR = 0.0476/0.1164 for 234 parameters and 2690 reflections with $I \geqslant 2\sigma(I)$, R/wR = 0.0751/0.1262 for all 3727 independent reflections measured in the range 8.80°–2θ–56.00°.

Crystal data for **12**: crystal dimension 0.19 × 0.36 × 0.60 mm^3; $C_{26}H_{25}FN_4O_4$, M_r = 476.50, triclinic space group $\bar{P}$; a = 9.4313(3), b = 10.9594(4), c = 12.4687(4) Å, α = 89.210(3), β = 87.665(2), γ = 70.720(3)°, V = 1215.49(7) Å^3; Z = 2; d_x = 1.302 g cm^{-3}; μ(MoKα) = 0.095 mm^{-1}; S = 0.803; R/wR = 0.0387/0.0846 for 324 parameters and 3035 reflections with $I \geqslant 2\sigma(I)$, R/wR = 0.0953/0.1048 for all 5856 independent reflections measured in the range 7.62°–2θ–56.00°.

Crystal data for **13**: crystal dimension 0.27 × 0.34 × 0.47 mm^3; $C_{16}H_{16}N_6O{\cdot}H_2O$, M_r = 326.36, monoclinic space group $P2_1/c$; a = 15.5183(5), b = 8.2078(2), c = 13.2945(4) Å, β = 107.517(3)°, V = 1614.81(8) Å^3; Z = 4; d_x = 1.342 g cm^{-3}; μ(MoKα) = 0.094 mm^{-1}; S = 0.954; R/wR = 0.0369/0.0627for 237 parameters and 2535 reflections with $I \geqslant 2\sigma(I)$, R/wR = 0.0984/0.1041 for all 3873 independent reflections measured in the range 7.40°–2θ–56.00°.

5.4. Cytostatic and antiviral activity assays

5.4.1. Cell culturing

The suspension cell lines L1210, Molt4/C8, and CEM were cultured in RPMI-1640 medium supplemented with 10% fetal bovine serum, 2 mM L-glutamine and 0.075% $NaHCO_3$ in a humidified atmosphere with 5% CO2 at 37 °C. The cell lines HeLa (cervical carcinoma), SW 620 (colon carcinoma), MiaPaCa-2 (pancreatic carcinoma), HEp-2 (larynx carcinoma), MCF-7 (breast carcinoma), SK-BR-3 (adenocarcinoma metastatic), and WI38 (normal diploid human fibroblasts), were cultured as monolayers and maintained in Dulbecco's modified Eagle's medium (DMEM) supplemented with 10% fetal bovine serum (FBS), 2 mM L-glutamine, 100 U/ml penicillin and 100 μg/ml streptomycin in a humidified atmosphere with 5% CO_2 at 37 °C.

5.4.2. Proliferation assays

The cytostatic activity against L1210, Molt4/C8, and CEM cells were measured in 200 μl-wells of a 96-well microtiter plate (initial cell number: 5–7.5 × 10^4 cells/well) essentially as originally described.[9]. After 48 (L1210) or 72 h (CEM, Molt4/C8), the tumor cell number was determined by a Coulter counter. For the antiproliferative assays, a panel of monolayer tumor cell lines (larynx carcinoma HEp-2, cervical carcinoma HeLa, breast carcinoma MCF-7, metastatic breast adenocarcinoma SK-BR-3, pancreatic carcinoma MiaPaCa-2, colon carcinoma SW 620, and human normal fibroblasts (WI38) were inoculated in standard 96-well microtiter plates on day 0, at 3000–6000 cells per well according to the doubling times of the specific cell line. Test agents were then added in five, 10-fold dilutions (1 × 10^{-8}–1 × 10^{-4} M) and incubated for another 72 h. The solvent (DMSO) was also tested for eventual inhibitory activity by adjusting its concentration to be the same as in the working concentrations (DMSO concentration never exceeded 0.1%). After 72 h of incubation, the cell growth rate was evaluated by performing the MTT assay: experimentally determined absorbance values were transformed into a cell percentage growth (PG) using the formulas proposed by NIH and described previously.[6] This method directly relies on control cells behaving normally at the day of assay because it compares the growth of treated cells with the growth of untreated cells in control wells on the same plate—the results are therefore a percentile difference from the calculated expected value.

The IC_{50} values for each compound were calculated from dose–response curves using linear regression analysis by fitting the test concentrations that give PG values above and below the reference value. If, however, all of the tested concentrations produce PGs exceeding the respective reference level of effect (e.g., PG value of 50) for a given cell line, the highest tested concentration is assigned as the default value (in the screening data report that default value is preceded by a '>' sign). Each test point was performed in quadruplicate in three individual experiments. Finally, the effects of the tested substances were evaluated by plotting the mean percentage growth for each cell type in comparison to control on dose–response graphs.

5.4.3. Antiviral activity assays

The antiviral assays, other than the anti-HIV assays, were based on inhibition of virus-induced cytopathicity in HEL [herpes simplex virus type 1 (HSV-1) (KOS), HSV-2 (G), vaccinia virus and vesicular stomatitis virus], Vero (parainfluenza-3, reovirus-1, Sindbis, Coxsackie B4, and Punta Toro virus), HeLa (vesicular stomatitis virus, Coxsackie virus B4, and respiratory syncytial virus) or MDCK [influenza A (H1N1; H3N2) and influenza B] cell cultures. Confluent cell cultures (or nearly confluent for MDCK cells) in microtiter 96-well plates were inoculated with 100 $CCID_{50}$ of virus (1 $CCID_{50}$ being the virus dose to infect 50% of the cell cultures). After a 1 h virus adsorption period, residual virus was removed, and the cell cultures were incubated in the presence of varying concentrations (200, 40, 8… μM) of the test compounds. Viral cytopathicity was recorded as soon as it reached completion in the control virus-infected cell cultures that were not treated with the test compounds. The methodology of the anti-HIV assays was as follows: human CEM cells (~3 × 10^5 cells/ml) were infected with 100 $CCID_{50}$ of HIV(III_B) or HIV-2(ROD)/ml and seeded in 200-μl wells of a microtiter

plate containing appropriate dilutions of the test compounds. After 4 days of incubation at 37 °C, HIV-induced giant cell formation was examined microscopically.

5.4.4. Cytotoxicity assays

Cytotoxicity measurements were based on the inhibition of HEL cell growth. HEL cells were seeded at a rate of 5×10^3 cells/well into 96-well microtiter plates and allowed to proliferate for 24 h. Then, medium containing different concentrations of the test compounds was added. After 3 days of incubation at 37 °C, the cell number was determined by a Coulter counter. The cytostatic concentration was calculated as the CC_{50}, the compound concentration required to reduce cell growth by 50% relative to the number of cells in the untreated controls. CC_{50} values were estimated from graphic plots of the number of cells (percentage of control) as a function of the concentration of the test compounds. Cytotoxicity was expressed as minimum cytotoxic concentration (MCC) or the compound concentration that causes a microscopically detectable alteration of cell morphology.

Acknowledgments

Support for this study was provided by the Ministry of Science, Education and Sports of the Republic of Croatia (Projects # 125-0982464-2922, # 098-0982464-2393, # 335-098-703532 and # 119-1193079-3069) and by the 'Geconcerteerde Onderzoeksacties' of the Katholieke Universiteit Leuven (project # 05/19). We thank Lizette van Berckelaer for excellent technical assistance in performing part of the antitumor cell activity assays, as well as Leen Ingels, Leentje Persoons, Frieda De Meyer, Vicky Broeckx, Anita Camps and Lies Vandenheurck for excellent technical assistance in performing the antiviral activity assays.

Supplementary data

Supplementary data associated with this article can be found, in the online version, at doi:10.1016/j.bmc.2010.07.035.

References and notes

1. De Clercq, E. *Adv. Virus Res.* **2009**, *73*, 1.
2. Krištafor, V.; Raić-Malić, S.; Cetina, M.; Kralj, M.; Šuman, L.; Pavelić, K.; Balzarini, J.; De Clercq, E.; Mintas, M. *Bioorg. Med. Chem.* **2006**, *14*, 8126.
3. Agrofoglio, L.; Suhas, E.; Farese, A.; Condom, R.; Challand, R. S.; Earl, R. E.; Guedj, R. *Tetrahedron* **1994**, *50*, 10611.
4. Ono, M.; Nishimura, K.; Tsubouchi, H.; Nagaoka, Y.; Tomioka, K. *J. Org. Chem.* **2001**, *66*, 8199.
5. Wu, Y.; Hong, J. H. *Il Farmaco* **2005**, *60*, 739.
6. Haines, D. R.; Tseng, C. K. H.; Marquez, V. E. *J. Med. Chem.* **1987**, *30*, 943.
7. Brakta, M.; Murthy, D.; Ellis, L.; Phadtare, S. *Bioorg. Med. Chem.* **2002**, *12*, 1489.
8. Priego, E. M.; Balzarini, J.; Karlsson, A.; Camarasa, M. J.; Perez-Perez, M. J. *Bioorg. Med. Chem.* **2004**, *12*, 5079.
9. Ashton, W. T.; Meurer, L. C.; Cantone, C. L.; Field, A. K.; Hannah, J.; Karkas, J. D.; Liou, R.; Patel, G. F.; Rerry, H. C.; Wagner, A. F.; Walton, E.; Tolman *J. Med. Chem.* **1988**, *31*, 2304.
10. Gazivoda, T.; Raić-Malić, S.; Krištafor, V.; Makuc, D.; Plavec, J.; Bratulić, S.; Kraljević-Pavelić, S.; Pavelić, K.; Naesens, L.; Andrei, G.; Snoeck, R.; Balzarini, J.; Mintas, M. *Bioorg. Med. Chem.* **2008**, *16*, 5624.
11. Cetina, M.; Nagl, A.; Krištafor, V.; Benci, K.; Mintas, M. *Cryst. Growth Des.* **2008**, *8*, 2975.
12. Cetina, M.; Džolić, Z.; Mrvoš-Sermek, D.; Hergold-Brundić, A.; Nagl, A.; Mintas, M. *J. Peptide Res.* **2004**, *63*, 391.
13. Bernstein, J.; Davis, R. E.; Shimoni, L.; Chang, N.-L. *Angew. Chem., Int. Ed. Engl.* **1995**, *34*, 1555.
14. Hunter, C. A.; Sanders, J. K. M. *J. Am. Chem. Soc.* **1990**, *112*, 5525.
15. Mrvoš-Sermek, D.; Cetina, M.; Krištafor, V.; Džolić, Z.; Mintas, M. *Z. Kristallogr.—New Cryst. Struct.* **2002**, *217*, 273.
16. Džolić, Z.; Krištafor, V.; Cetina, M.; Nagl, A.; Hergold-Brundić, A.; Mrvoš-Sermek, D.; Burgemeister, T.; Grdiša, M.; Slade, N.; Pavelić, K.; Balzarini, J.; De Clercq, E.; Mintas, M. *Nucleosides Nucleotides Nucleic Acids* **2003**, *22*, 373.
17. Oxford Diffraction, Xcalibur CCD System, CrysAlisPro, Oxford Diffraction Ltd, Abingdon, England.
18. Sheldrick, G. M. *Acta Crystallogr., Sect. A* **2008**, *64*, 112.
19. Spek, A. L. *J. Appl. Crystallogr.* **2003**, *36*, 7.